International Journal of Radiation Oncology biology • physics

www.redjournal.org

Physics Contribution

A Mechanism-Based Approach to Predict the Relative Biological Effectiveness of Protons and Carbon Ions in Radiation Therapy

Malte C. Frese, Ph.D.,[*,†] Victor K. Yu, M.S.,[*] Robert D. Stewart, Ph.D.,[‡] and David J. Carlson, Ph.D.[*]

[*]Department of Therapeutic Radiology, Yale University School of Medicine, New Haven, Connecticut; [†]Department of Medical Physics in Radiation Oncology, German Cancer Research Center, Heidelberg, Germany; and [‡]Department of Radiation Oncology, University of Washington, Seattle, Washington

Received Mar 11, 2011, and in revised form Jun 16, 2011. Accepted for publication Jun 17, 2011

Summary

The physical pattern of energy deposition and the enhanced relative biological effectiveness (RBE) of heavy ions compared to photons offers unique, and not fully understood, opportunities to improve the efficacy of radiation therapy. In this work, an approach to predict proton and carbon ion RBE in representative spread-out Bragg peaks is derived using the mechanistic repair-misrepair-fixation (RMF) model. Treatments that exploit the combined physical and radiobiologic properties of heavy ions have the potential to provide much higher levels of tumor control and improved normal tissue sparing than photon treatments.

Purpose: The physical and potential biological advantages of proton and carbon ions have not been fully exploited in radiation therapy for the treatment of cancer. In this work, an approach to predict proton and carbon ion relative biological effectiveness (RBE) in a representative spread-out Bragg peak (SOBP) is derived using the repair-misrepair-fixation (RMF) model.

Methods and Materials: Formulas linking dose-averaged linear-quadratic parameters to DSB induction and processing are derived from the RMF model. The Monte Carlo Damage Simulation (MCDS) software is used to quantify the effects of radiation quality on the induction of DNA double-strand breaks (DSB). Trends in parameters α and β for clinically relevant proton and carbon ion kinetic energies are determined.

Results: Proton and carbon ion RBE are shown to increase as particle energy, dose, and tissue α/β ratios decrease. Entrance RBE is $\sim$1.0 and $\sim$1.3 for protons and carbon ions, respectively. For doses in the range of 0.5 to 10 Gy, proton RBE ranges from 1.02 (proximal edge) to 1.4 (distal edge). Over the same dose range, the RBE for carbon ions ranges from 1.5 on the proximal edge to 6.7 on the distal edge.

Conclusions: The proposed approach is advantageous because the RBE for clinically relevant particle distributions is guided by well-established physical and biological (track structure) considerations. The use of an independently tested Monte Carlo model to predict the effects of radiation quality on DSB induction also minimizes the number of *ad hoc* biological parameters that must be determined to predict RBE. Large variations in predicted RBE across an SOBP may produce undesirable biological hot and cold spots. These results highlight the potential for the optimization of physical dose for a uniform biological effect. © 2012 Elsevier Inc.

Keywords: Carbon ions, Cell survival, Protons, RBE, Repair-misrepair-fixation (RMF) model

Reprint requests to: David J. Carlson, Ph.D., Department of Therapeutic Radiology, Yale University School of Medicine, New Haven, CT 06520-8040. Tel: (203) 200-2018; Fax: (203) 688-8682; E-mail: david.j.carlson@yale.edu

This work was supported by American Cancer Society grant IRG-58-012-52 (to D.J.C.).

Conflict of interest: none.

Acknowledgment—The authors thank Mr. Joo Han Park for providing secondary electron spectra for 200 kVp X-rays.

Int J Radiation Oncol Biol Phys, Vol. 83, No. 1, pp. 442–450, 2012
0360-3016/$ - see front matter
doi:10.1016/j.ijrobp.2011.06.1983

Introduction

Radiotherapy with charged particles has gained much interest recently. Numerous new proton and carbon ion therapy centers are being built around the world. The interest in particles is fueled by the nature of their physical interactions with matter, which allows highly conformal dose distributions while at the same time reducing the volume of normal tissue irradiated. Although the physical characteristics of particles are well understood, models to predict the complex sequence of molecular, cellular, and tissue responses to initial damage are less well developed. Decades of laboratory and clinical experience provide evidence that the same levels of tumor control can be achieved with proton doses that are 10% to 20% lower than the doses required with high-energy photons. That is, protons have a relative biological effectiveness (RBE) of about 1.1 to 1.2 compared to high-energy photons (1). With the larger RBE of a more massive ion, the identification of a biologically optimal dose distribution becomes more challenging. A more accurate assessment of the potential opportunities and risks of using particles in radiation therapy will only be possible through an improved understanding of the underlying mechanisms of biological response.

Protons are currently the most frequently used particles for radiotherapy. In clinical practice, a constant RBE value of 1.1 is recommended (1, 2), despite some evidence that exploiting variations in RBE within and near treated volumes may enhance treatment outcome (3). There is no doubt that a spatially invariant RBE within target volumes is not appropriate for carbon ions (4).

In this work, we develop a mechanism-based approach to predict spatially varying proton and carbon ion RBE values for representative spread-out Bragg peaks (SOBP). First, the repair-misrepair-fixation (RMF) model (5) is used to develop formulas explicitly linking radiosensitivity parameters in the widely used linear-quadratic (LQ) survival model to the induction and biological processing of DNA double-strand breaks (DSB). To minimize the number of *ad hoc* adjustable parameters, the published Monte Carlo Damage Simulation (MCDS) software (available at http://faculty.washington.edu/trawets/mcds/) is used to predict the effects of radiation quality on DSB induction (6, 7). A multiscale modeling approach such as this is potentially advantageous because the RBE for clinically relevant particle distributions is guided by well-established physical and biological considerations. The models and methods are used to examine the impact of tissue radiosensitivity on RBE for monoenergetic heavy ions as well as more clinically relevant proton and carbon ion SOBP. Throughout this article the term RBE refers to that for cell survival.

Methods and Materials

The biological effects of charged particles on tissues depend on both physical characteristics of the particle beam and tissue-specific biological parameters. In the following sections, we first discuss how physical beam parameters such as dose and stopping power are calculated. This is followed by sections on the biological models and the calculation of tissue specific parameters.

Physical characteristics of particle beams

An analytical power law for the range of protons in water as a function of energy is used to describe the physical characteristics of particle beams (8). This power law has been used successfully to calculate physical dose (9) and linear energy transfer (LET) (10) for protons. According to the power law, the range, R, of a proton (denoted by index p) is given by

$$R = k_p E^p, \tag{1}$$

where E is the kinetic energy of the proton. The constants $k_p = 0.0022\ \mathrm{MeV}^{-p}$ and $p = 1.77$ are given by Bortfeld (9). Equation 1 can be applied to more massive ions of charge Z and mass A if multiplied by A^{1-p}/Z^2 (11). The kinetic energy of an ion in depth, z, is therefore given by

$$E(z) = k_q^{-1/p}(R_0 - z)^{1/p} \tag{2}$$

where R_0 is the initial range of the ion and $k_q = A^{1-p}/Z^2 \cdot k_p$. The index q denotes a charged particle with radiation quality q. Taking the negative derivative of Eq. 2 with respect to depth yields stopping power S

$$S(z) = -\frac{dE(z)}{dz} = \frac{1}{p} k_q^{-1/p}(R_0 - z)^{1/p-1}. \tag{3}$$

These modified methods are used to calculate physical dose and stopping power for primary ions. The contributions of secondary particles created in the patient are neglected.

The Repair-Misrepair-Fixation (RMF) model

For a single dose of radiation delivered over a short time interval, the LQ model is commonly used to relate absorbed dose, D, to biological effect, $\mathcal{E}$, through two radiosensitivity parameters (α and β):

$$\mathcal{E} = \alpha D + \beta D^2 = \alpha D\left(1 + \frac{D}{\alpha/\beta}\right). \tag{4}$$

In general, α and β depend on many factors, including the nature of the irradiated tissue, oxygen concentration, and radiation type and quality. The literature contains estimates of α and β for cells irradiated *in vitro* under well-defined reference conditions. Estimates of α and β values have also been derived from *in vivo* (animal) experiments and from clinical data for selected tumor types and normal tissues. A major challenge for any translational modeling effort is to leverage knowledge of well-understood biological mechanisms gleaned from experiments carried out under controlled laboratory conditions to improve the accuracy and reliability of predictions for alternate experimental and/or *in vivo* conditions.

In the RMF model (5), reproductive cell death by mitotic catastrophe, apoptosis, or other cell death modes is explicitly linked to DSB induction and processing. In particular, we have shown that the effects of radiation quality, q, on α and β for particles with a stopping power up to at least 100 to 150 keV/μm can be modeled using

$$\alpha(q) = \theta\Sigma(q) + \kappa\bar{z}_F(q)\Sigma^2(q), \tag{5}$$

and

$$\beta(q) = (\kappa/2)\Sigma^2(q). \tag{6}$$

Here, Σ is the initial number of DSB per Gray per giga base pair ($\mathrm{Gy}^{-1}\ \mathrm{Gbp}^{-1}$), $\bar{z}_F$ is the frequency-mean specific energy (Gy), and θ and κ are tumor- or tissue-specific parameters related to the biological processing of initial DSB. For a spherical water target of diameter d, the frequency-mean specific energy can be approximated by

$$\bar{z}_F(q) = 0.204 \cdot \frac{S}{d^2}. \tag{7}$$

An attractive feature of Eqs. 5 and 6 is that estimates of α and β for any particle type, including electrons and photons, are determined by a well-defined, purely physical parameter that is the same *in vitro* and *in vivo* ($\bar{z}_F$), two biological parameters (θ and κ) that are tissue-specific but independent or a weak function of radiation quality, and a biological parameter (Σ) that is a strong function of radiation quality (track structure) but is approximately the same *in vitro* and *in vivo* and among all mammalian cells. Sophisticated Monte Carlo models are also available to predict trends in Σ with radiation quality (see ref. 6 and references therein). All reported results are based on estimates of Σ obtained with the MCDS (6, 7).

For a reference radiation x with known radiation sensitivity parameters α_x and β_x, the radiation quality-dependent LQ parameters are given by

$$\alpha(q)=\frac{\Sigma(q)}{\Sigma_x}\left[\alpha_x+2\frac{\beta_x}{\Sigma_x}(\Sigma(q)\bar{z}_F(q)-\Sigma_x\bar{z}_{F,x})\right], \tag{8}$$

and

$$\beta(q)=\left(\frac{\Sigma(q)}{\Sigma_x}\right)^2\beta_x. \tag{9}$$

Equations 8 and 9 provide a convenient formalism to relate published radiosensitivity parameters for photons and other radiations with low LET to radiosensitivity parameters for other particle types, including protons and carbon ions.

Determination of LQ parameters in a pristine Bragg peak

Particle beams used in clinical radiotherapy have an energy spectrum that cannot be neglected. The two main components are the initial energy spectrum of the accelerator and contributions of stochastic interactions of particles in matter that give rise to so-called straggling. Assuming that both components of the particle distribution have a Gaussian spectrum (9), the width of the combined spectrum can be obtained by quadratic addition of the individual widths. Particles of different kinetic energies and, hence, different RBE values, contribute to the total physical dose deposited at any given location. Within the framework of the LQ model, the synergistic effects of radiation may be incorporated into RBE calculations by computing the dose-averaged parameters α_D and $\sqrt{\beta_D}$ (12, 13). Zaider and Rossi (12) described the effect of two overlapping radiations of different quality. Wilkens and Oelfke (13) extended this approach to a discrete set of N overlapping radiation beams:

$$\alpha_D=\frac{\left(\sum_{i=1}^{N}\alpha_i D_i\right)}{D} \text{ and } \sqrt{\beta_D}=\frac{\left(\sum_{i=1}^{N}\sqrt{\beta_i}D_i\right)}{D} \tag{10}$$

Here, the total dose D is obtained by the equation $D=\sum_{i=1}^{N}D_i$. We extend this approach to an energy spectrum by using the same method that Wilkens and Oelfke (10) used to calculate dose-averaged LET for a proton beam with an energy spectrum.

As energy, range, and depth in tissue are directly correlated (8), a spectrum of energies can also be expressed as a spectrum of ranges or depths. The latter is used here so that dose and dose-averaged radiation sensitivity parameters α_D and β_D are presented as a function of depth:

$$\alpha_D(z)=\frac{\int_{-\infty}^{R_0}dz'\,\alpha(z')\phi_{z'}(z)S(z')}{\int_{-\infty}^{R_0}dz'\,\phi_{z'}(z)S(z')} \tag{11}$$

and

$$\sqrt{\beta_D}(z)=\frac{\int_{-\infty}^{R_0}dz'\,\sqrt{\beta}(z')\phi_{z'}(z)S(z')}{\int_{-\infty}^{R_0}dz'\,\phi_{z'}(z)S(z')}. \tag{12}$$

Here, $\phi_{z'}(z)$ is the Gaussian distribution of particles about depth z that have the same stopping power $S(z')$ as monoenergetic particles would have at depth z'. If we apply Eqs. 11 and 12 to Eqs. 5 and 6, respectively, we obtain

$$\alpha_D(z)=\theta\langle\Sigma(z)\rangle_D+\kappa\langle\bar{z}_F(z)\Sigma(z)^2\rangle_D \tag{13}$$

and

$$\beta_D(z)=\frac{\kappa}{2}\langle\Sigma(z)\rangle_D^2. \tag{14}$$

Determination of LQ parameters in an SOBP

To deposit homogenous doses in large volumes, many Bragg peaks of different initial energies are overlapped to create an SOBP. Following Eq. 10, the biological effect $\mathcal{E}$ of N Bragg peaks is

$$\mathcal{E}=\alpha_D D+\beta_D D^2=\sum_{i=1}^{N}\alpha_i D_i+\left(\sum_{i=1}^{N}\sqrt{\beta_i}D_i\right)^2. \tag{15}$$

Index i denotes the contribution from Bragg peak i. RBE-weighted doses (RWD) are calculated to compare the effectiveness of different radiation modalities (2). RBE is defined as the ratio of a low-LET reference dose to a dose with radiation quality q that produces the same biological effect:

$$RBE=\frac{\sqrt{\alpha_x^2+4\beta_x D(\alpha_D+\beta_D D)}-\alpha_x}{2\beta_x D} \tag{16}$$

Incorporating Eqs. 8 and 9 into Eq. 16 gives

$$RBE=\frac{1}{2D}\left[\sqrt{\left[\left(\frac{\alpha}{\beta}\right)_x+2D\frac{\langle\Sigma\rangle_D}{\Sigma_x}\right]^2+\frac{8D}{\Sigma_x^2}\left(\langle\bar{z}_F\Sigma^2\rangle_D-\bar{z}_{F,x}\Sigma_x\langle\Sigma\rangle_D\right)}-\left(\frac{\alpha}{\beta}\right)_x\right]. \tag{17}$$

Within this model, RBE depends on $(\alpha/\beta)_x$ but is independent of α_x.

Low-LET reference radiosensitivity parameters

As indicated by Eq. 17, RBE depends on radiation quality through the $\bar{z}_F$ and Σ parameters, absorbed dose, and $(\alpha/\beta)_x$. Because dose, $\bar{z}_F$, and Σ are estimated using physical models or an independently tested Monte Carlo simulation, our approach predicts that RBE varies among tumor types and tissues solely because of differences in $(\alpha/\beta)_x$. For this reason, multiple sets of low-LET radiosensitivity parameters (Table 1) are examined. For comparison with measured trends in radiosensitivity (14), we use the respective low-LET reference parameters for each cell line. The

Table 1 Low-LET reference parameters derived from published *in vitro* and *in vivo* data

Cell or tissue type	α_x (Gy^{-1})	β_x (Gy^{-2})	$(\alpha/\beta)_x$ (Gy)	θ (Gbp)	κ (Gbp^2)	θ/κ (Gbp^{-1})*	Ref. rad.	Reference/study
T1	0.0305	0.0585	0.52	0.0033	1.6×10^{-3}	2.15	200 kVp	Furusawa *et al.* (14)
HSG	0.313	0.0615	5.1	0.0359	1.6×10^{-3}	21.98	200 kVp	Furusawa *et al.* (14)
V79	0.184	0.020	9.2	0.0211	5.3×10^{-4}	39.82	200 kVp	Furusawa *et al.* (14)
Chordoma	0.1	0.050	2	0.0121	1.5×10^{-3}	8.25	Co-60	Kramer and Scholz (4)
Prostate	0.15	0.048	3.1	0.0181	1.4×10^{-3}	12.79	Co-60	Carlson *et al.* (15)
Head and neck	0.25	0.025	10	0.0302	7.3×10^{-4}	41.33	Co-60	Girinsky *et al.* (16); Stuschke and Thames (17)

Abbreviations: Ref. rad. = reference radiation; HSG = human submandibular gland cell line.
* θ and κ are calculated based on the reference parameter values using Eqs. 5 and 6, respectively.

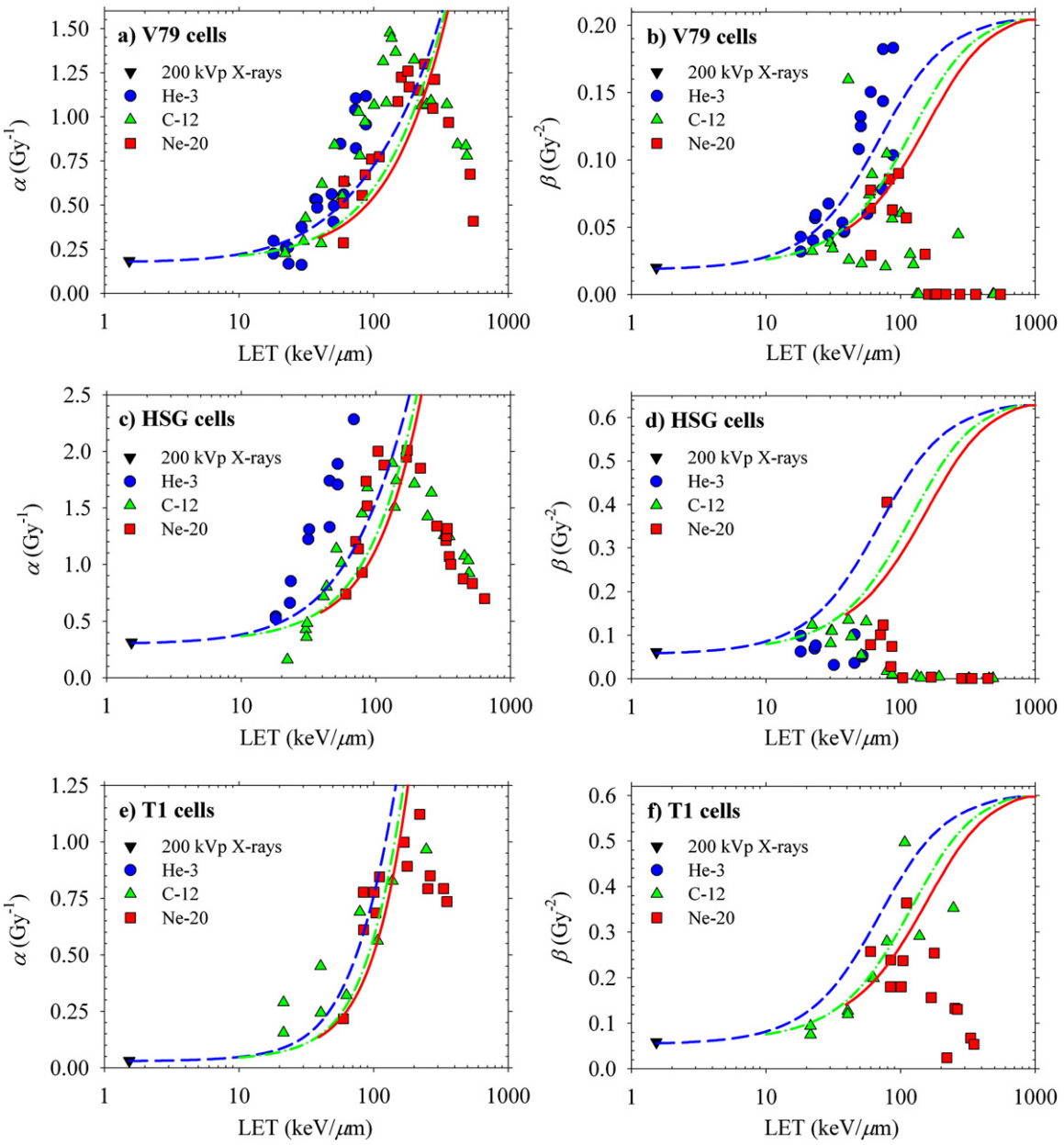

Fig. 1. Predictions are shown for α and β as functions of particle LET for helium (He-3, dashed lines), carbon (C-12, dash-dotted lines), and neon (Ne-20, solid lines) ions based on a single reference point (triangles) for 200 kVp X-rays. Symbols show measured values (14) derived from cell survival data.

reference DSB yield $\sum_{200\ kVp} = 8.68\ Gy^{-1}\ Gbp^{-1}$ for 200 kVp X-rays was simulated using MCDS with a secondary electron spectrum obtained from MCNP (Monte Carlo N-Particle Transport Code). The frequency-mean specific energy was calculated for $S_{200\ kVp} = 1.53\ keV/\mu m$. For all other calculations, we use three additional reference data sets representing chordoma (4), prostate (15), and head and neck tumors (16, 17), which cover a large range of $(\alpha/\beta)_x$ observed *in vivo*. To calculate the RMF model parameters θ and κ for clinical conditions, we assume that all reference radiosensitivity parameters were obtained with cobalt-60 (^{60}Co) irradiation. Including a secondary electron spectrum (18), we simulated the reference DSB yield $\Sigma_x = 8.27\ Gy^{-1}Gbp^{-1}$ with a reference stopping power of $S_x = 0.36\ keV/\mu m$. To represent the nucleus of a cell, we use a diameter of 5 μm in Eq. 7.

Results

Predicting trends in intrinsic radiosensitivity with particle LET

Figure 1 shows radiosensitivity parameters predicted for V79, HSG, and T1 cells for three different ion species (helium-3, carbon-12, and neon-20) over a wide range of LET values. Reference radiosensitivity parameters (Table 1) were measured using 200 kVp X-rays (14). Model predictions were calculated using Eqs. 5 and 6. DSB yields were obtained with the MCDS model, and the physical properties of the monoenergetic particles were calculated with analytical functions. Predictions are contrasted with measured data points published by Furusawa *et al.* (14). The model predicts the same trends as those in the measured data but tends to underestimate α and overestimate β for lower LET values. Measured parameters reach their respective maximum between 100 keV/μm and 250 keV/μm, depending on the ion species, while the RMF model predicts increasing parameters beyond this point, as both Σ and $\bar{z}_F$ increase with LET. For LET values that exceed $\sim$150 keV/μm, the model overpredicts measured α and β values.

Physical and radiobiological properties of a pristine Bragg peak

Modern particle therapy facilities use narrow, pencil beam scanning. Figure 2 shows physical and radiobiological properties of a proton and a carbon ion pencil beam with a range of 15 cm in water, assuming the radiosensitivity of chordoma tissue. All calculations include depth straggling and an additional depth spectrum created by a 3 mm ripple filter (19). Dose and dose-averaged LET (LET_d) values were calculated using modified analytical models (9, 10). DSB yields are dose-averaged, *i.e.*, an average value of the DSB yield for monoenergetic particles. Parameters α_D and β_D were calculated using Eqs. 13 and 14, respectively, and are determined primarily by the DSB yield. This is consistent with results shown in Figure 2. All three curves show a similar shape with a plateau in the entrance channel of the beam. For protons, parameters in the entrance channel equal the reference parameters ($\alpha_x = 0.1\ Gy^{-1}$, $\beta_x = 0.05\ Gy^{-2}$). For carbon ions, they are increased by $\sim$ 50%. All values rise sharply as the depth approaches the Bragg peak. The significance of the maximum values must be carefully considered as they are associated with very low doses. Values that coincide with the maximum dose are likely to have greater clinical relevance. At the maximum dose, we observe values of $\alpha_D = 0.16\ Gy^{-1}$ for protons and $\alpha_D = 2.31\ Gy^{-1}$ for carbon ions, *i.e.*, an increase by a factor of 1.5 and 15, respectively. Similarly, β_D increases to values of $0.08\ Gy^{-2}$ and $0.38\ Gy^{-2}$ for protons and carbon ions, respectively.

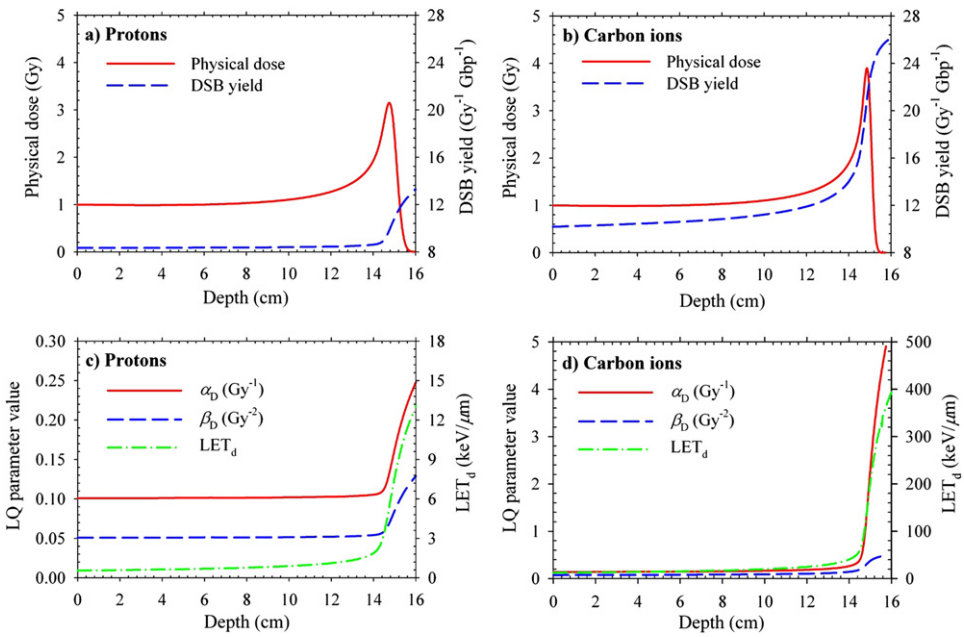

Fig. 2. Physical and biological properties of proton and carbon ion pristine Bragg peaks are shown. Dose and LET values were calculated using analytical models. DSB yields were simulated with the MCDS algorithm. Values for α_D and β_D were calculated for chordoma tissue using Eqs. 13 and 14, respectively. All calculations include a Gaussian particle spectrum.

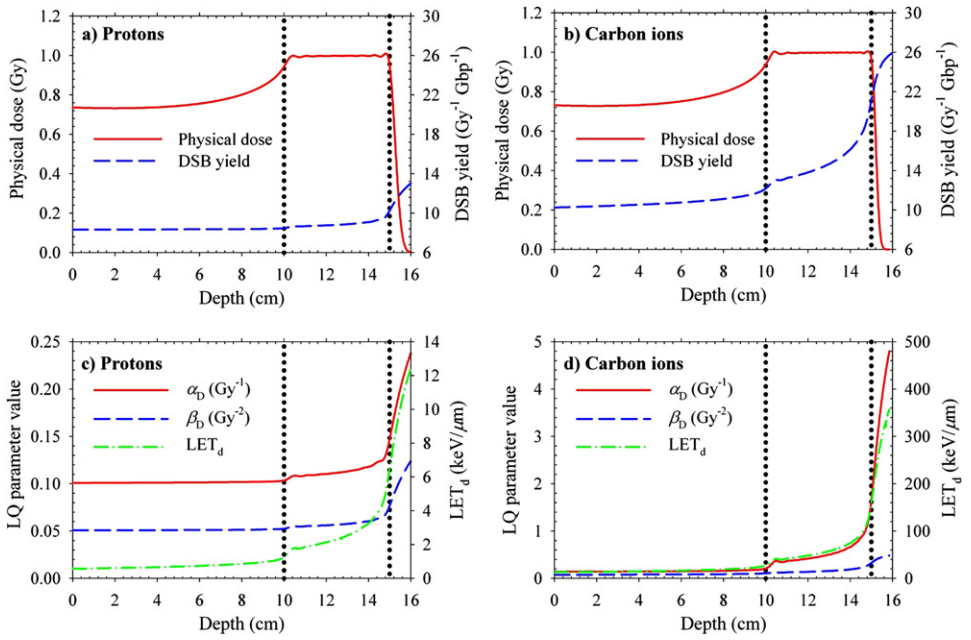

Fig. 3. Physical and biological properties of a proton and carbon ion SOBP are shown. Dotted lines show proximal ($z = 10$ cm) and distal edges ($z = 15$ cm) of the SOBP. All quantities except physical dose were calculated from the contribution of individual pristine Bragg peaks using Eq. 10, which was adapted for DSB yield and LET.

Physical and radiobiological properties of SOBP

Figure 3 shows physical and radiobiological properties of a proton and a carbon SOBP consisting of 17 pencil beams with residual ranges spaced 3 mm apart. The fluence of the pencil beams is optimized such that a constant absorbed dose of 1 Gy is deposited from the proximal edge of the SOBP at 10 cm water equivalent depth to its distal edge at 15 cm. Dose-averaged values of α_D, β_D, the DSB yield, and LET are calculated from the contributions of the individual pencil beams. Apart from the absorbed dose, all quantities are nearly constant for depths of < 10 cm and exhibit the same trends in the SOBP and past the distal edge. At the proximal edge, where the first Bragg peak is located, each measure rises to a second plateau and then rises slowly across the width of the SOBP. Approaching the distal edge of the SOBP, all quantities rise steeply as they are dominated by the Bragg peak with the greatest range. Dominated by the rise in DSB yield, α_D and β_D increase by $\sim$ 10 % for protons and $\sim$ 100 % for carbon ions. Across the SOBP, α_D increases by another 50 % for protons and $>$ 500 % for carbon ions. The increase in β_D is smaller as it depends only on the DSB yield and not on particle LET. The relative rise of the latter is considerably steeper at the proximal edge of the SOBP.

Influence of $(\alpha/\beta)_x$ on RBE

According to Eq. 17, the tissue dependence of RBE is reflected only in the $(\alpha/\beta)_x$ value of the reference parameter set. This dependence is shown in Figure 4, where the RWD of three tissues with different $(\alpha/\beta)_x$ values (Table 1) are compared for an SOBP with a constant absorbed dose of 1 Gy. RWD is shown to increase with a decrease in $(\alpha/\beta)_x$. Differences in RBE estimates are as large as 25 % for carbon ions and smaller than 5 % for protons.

Low doses have a high impact on the RBE

Figure 5 shows predicted RBE values in SOBPs optimized for constant absorbed doses ranging from 0.1 to 10 Gy. RBE estimates are nearly independent of absorbed doses $>$ 2.5 Gy. The

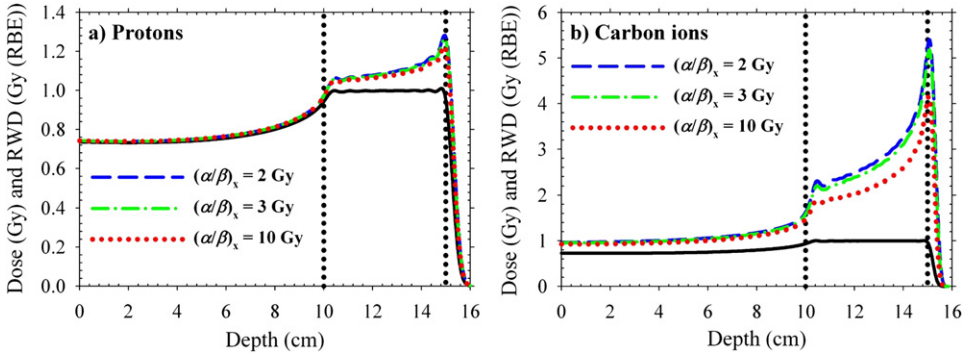

Fig. 4. Physical (solid line) and RBE-weighted (RWD) dose for representative clinical SOBPs in proton and carbon ion radiotherapy. Dashed, dashed-dotted, and dotted lines represent RWD for chordoma, prostate, and head and neck cancer, respectively.

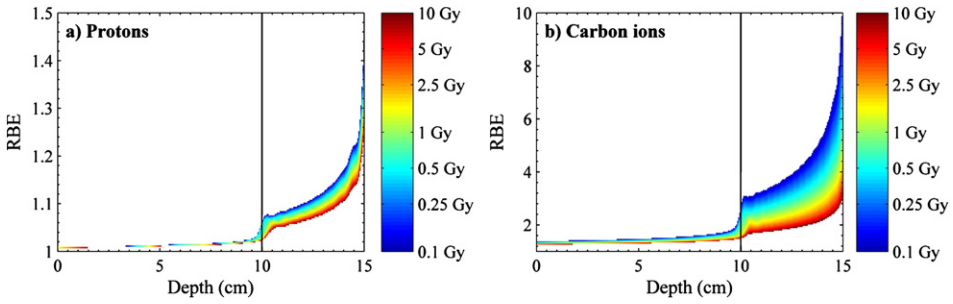

Fig. 5. RBE values for chordoma tissue in proton and carbon ion SOBPs ranging from 10 cm (solid black line) to 15 cm for physical doses ranging from $0.1 - 10$ Gy. Increasing RBE estimates correspond with decreasing dose.

carbon ion RBE for lower doses depends up to 50 % on the absorbed dose. For protons, this influence is on the order of 5 %. For particles with higher $(\alpha/\beta)_x$ values, the impact of dose on RBE estimates is smaller (data not shown). No significant dose dependence is observed outside of the SOBP. Table 2 shows RBE values for cell killing for protons and carbon ions for a range of tissue radiosensitivities and physical doses. The average RBE of protons is $\sim$ 1.1 and is nearly independent of dose and $(\alpha/\beta)_x$, while the average carbon ion RBE ranges from $2.0 - 4.5$ for $(\alpha/\beta)_x = 2$ Gy and from $1.9 - 2.5$ for $(\alpha/\beta)_x = 10$ Gy.

Optimizing physical dose to achieve a constant biological effect

In Figures 2 to 5, a constant physical dose is deposited across the volume covered by the SOBP. Ideally, the true clinical objective in radiotherapy is to deliver a constant biological effect across the tumor volume. Employing the method developed by Wilkens and Oelfke (13), we optimized the RBE-weighted dose for protons and carbon ions for a constant RWD of 3 Gy (RBE). Figure 6 shows a relatively constant RWD in the SOBP and the underlying physical doses for both protons and carbon ions. In order to keep the RWD constant across the SOBP, the physical dose must decrease from the proximal to the distal edge. Here, the increase of the RBE with LET reduces the required dose, which in turn increases the RBE. Although this effect is more pronounced for carbon ions, due to lower doses and higher LET, it can also be observed for protons. Comparing the RBE-weighted doses of protons and carbon ions, we found that the entrance to plateau ratio is approximately 2:3 for protons and 1:3 for carbon ions.

Table 2 RBE values for cell killing for protons and carbon ions for a range of tissue radiosensitivities and physical doses

	RBE (α/β = 2 Gy)			RBE (α/β = 10 Gy)		
Dose (Gy)	Proximal	Distal	Avg	Proximal	Distal	Avg
Protons						
0.1	1.06	1.44	1.13	1.04	1.28	1.09
0.5	1.06	1.38	1.12	1.04	1.28	1.09
1	1.03	1.34	1.11	1.03	1.27	1.09
2	1.03	1.30	1.10	1.03	1.27	1.09
5	1.02	1.27	1.09	1.02	1.26	1.08
10	1.02	1.26	1.08	1.02	1.25	1.08
Carbon ions						
0.1	2.69	10.85	4.48	1.81	5.11	2.49
0.5	2.26	6.74	3.32	1.77	4.59	2.39
1	1.83	5.38	2.82	1.62	4.21	2.29
2	1.60	4.35	2.43	1.53	3.79	2.17
5	1.52	3.44	2.10	1.50	3.28	2.02
10	1.49	3.04	1.96	1.48	2.99	1.93

Estimates are shown for the proximal edge (z = 10 cm), distal edge (z = 15 cm), and target average for a clinical Bragg peak spread of 5 cm.

Discussion

Predicting radiobiological parameters

In its current form, the RMF model tends to overpredict α for LET values above $\sim$150 keV/μm (Fig. 1). This discrepancy can be attributed to both potential limitations of the RMF model and neglected nuclear fragments. Limitations of the RMF model have been discussed elsewhere (5), and model improvements are currently being investigated. The potential overprediction of radiosensitivity for LET $>$ $\sim$150 keV/μm does not affect the proton calculations, as the LET of therapeutic protons is well below this limit (Figs. 2c and 3c). This limitation will introduce uncertainty in the prediction of carbon ion RBE as LET values exceed 150 keV/μm at the position of the Bragg peak (Fig. 2d). The proposed approach is therefore expected to overpredict the carbon ion RBE at the distal edge of the SOBP.

The effects of nuclear fragments and secondary protons are neglected in this work. Secondary protons should not be neglected when calculating the LET of intensity-modulated proton fields (20). The clinical significance of secondary protons for our predictions will be investigated in future studies. For heavier ions, most fragments have a lower charge squared-to-mass ratio than the primary ions and therefore a lower LET and longer range. A real beam with a secondary particle spectrum may therefore produce a reduced biological effect for the same dose compared to the single particle beam assumed here.

Trends in β and potential reasons for the deviations of measured and predicted data have been discussed elsewhere (5, 21). We studied the influence of β by replacing it with a constant value equal to the reference parameter (data not shown). In chordoma, we observed differences in the RBE of $1\% - 10$ % for protons and $10\% - 20$ % in carbon ions across the SOBP. This is in agreement with recently published findings that the correct choice of β is critical for predicting outcome in proton therapy (21).

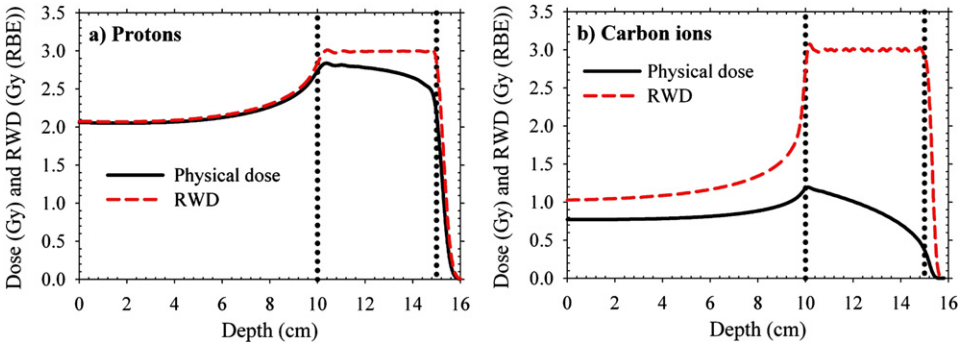

Fig. 6. Physical doses for proton and carbon ion SOBP required to yield a constant RBE-weighted dose (RWD) of 3 Gy (RBE) are shown. Each SOBP consists of pristine Bragg peaks with fluences optimized to yield a constant RWD.

Good agreement between the proposed approach and measured data can also be found in the observed proton RBE values. The average proton RBE of 1.1 reported for a wide range of tissues and doses (Table 2 and Figs. 4 and 5) compares well to the accumulated published data (1). For carbon ions, a greater change in RBE across the SOBP is predicted than that obtained using the local effect model in clinically implemented settings (4, 22). The local effect model used at the HIT facility in Heidelberg for patient treatment predicts an RBE range of $3-3.5$ across a SOBP (23), which is a significantly smaller range than the $1.8-5.4$ reported here. Similar trends in α across a SOBP are found in the recent application of the microdosimetric kinetic model for carbon ion treatment planning (24). The microdosimetric kinetic model predicts a decrease in α beyond the distal edge of the SOBP, which may be due to more sophisticated modeling of proximity or overkill effects as well as limitations of using an approximate analytical formula to estimate frequency-mean specific energy.

Radiosensitivity of different tissues

Our modeling approach predicts that RBE depends only on the $(\alpha/\beta)_x$ value. Tissues were purposely chosen to cover a large range of biologically plausible $(\alpha/\beta)_x$ values. A large dependence on tissue type was not observed for protons, while the maximum RBE for carbon ions at different points in the SOBP varied by more than 20 % among tissue types. This implies that a correct choice of tissue parameters is more crucial for carbon ions than for protons. With our model, assigning a low $(\alpha/\beta)_x$ value to a tumor target that actually has a high $(\alpha/\beta)_x$ value overestimates RBE (and RWD) and may result in plans that deliver a physical dose lower than necessary to achieve tumor control. The converse argument can be made for normal tissues. To ensure adequate tumor control without undue damage to normal tissues, it may be prudent to optimize carbon ion plans by using a large $(\alpha/\beta)_x$ for the tumor and a small $(\alpha/\beta)_x$ for normal tissues.

Influence of dose on RBE predictions

We observed a considerable dose effect for carbon ions for doses < 2.5 Gy. Most carbon ion treatments with conventional fractionation schemes employ absorbed doses in the range of $0.5-1$ Gy (Fig. 6), corresponding to RWDs of $\sim 2-4$ Gy (RBE). The dose dependence is on the same order of magnitude as the change of RBE with radiation quality. Wilkens and Oelfke (23) reported the RBE outside an SOBP peak may be higher than within due to this dose effect. In contrast to their findings, we predict a small dose effect in the normal tissue outside a SOBP (Fig. 5). This difference may be a result of neglecting nuclear fragments and considering only a single-field SOBP.

Optimization of RBE-weighted dose

There is no debate regarding the necessity for the optimization of physical dose to obtain a constant RBE-weighted dose in carbon ion therapy. The results of this study strongly suggest that this approach should also be considered in proton radiotherapy. Our simulations show that RBE-weighted dose can change by up to 30% across a 5 cm SOBP. RBE values can consistently deviate by more than 10% from the assumed nominal value of 1.1 in some parts of the SOPB regardless of the tissue and absorbed dose. We also show that the RBE-weighted proton dose is relatively insensitive to tissue radiosensitivity. The potential errors in predicting RBE introduced by assuming the wrong tissue radiosensitivity are likely smaller than the errors introduced by assuming a constant RBE of 1.1.

Conclusions

The proposed approach allows for the quantitative evaluation of the effect of particle LET on DSB induction and cell death in proton and carbon ion radiotherapy. Results of this study indicate the potential for biological hot and cold spots within the SOBP in both proton and carbon ion radiotherapy. For carbon ions, the correct choice of tissue reference parameters is crucial for the prediction of accurate RBE values. The dependence of RBE estimates on reference parameters is less critical for protons. The development of biologically motivated models of RBE results in an enhanced understanding of the biophysical mechanisms underlying cell killing in X-ray and particle therapy, as well as the determination of RBE estimates that can be practically used in charged particle radiotherapy to optimize physical dose for a uniform biological effect. The approach proposed in this paper allows for a robust inclusion of oxygen effects by correcting the DSB yields for oxygen concentration in the MCDS algorithm. Future work is under way to investigate the impact of tumor hypoxia on the relative effectiveness of proton, carbon ion, and X-rays.

References

1. Paganetti H, Niemierko A, Ancukiewicz M, *et al*. Relative biological effectiveness (RBE) values for proton beam therapy. *Int J Radiat Oncol Biol Phys* 2002;53:407–421.

2. ICRU. Prescribing, recording, and reporting proton-beam therapy. ICRU Report 78; International Commission on Radiation Units & Measurements (ICRU), Bethesda, MD 2007.
3. Frese MC, Wilkens JJ, Huber PE, *et al*. Application of constant vs. variable relative biological effectiveness in treatment planning of intensity-modulated proton therapy. *Int J Radiat Oncol Biol Phys* 2011;79:80−88.
4. Kramer M, Scholz M. Treatment planning for heavy-ion radiotherapy: Calculation and optimization of biologically effective dose. *Phys Med Biol* 2000;45:3319−3330.
5. Carlson DJ, Stewart RD, Semenenko VA, *et al*. Combined use of Monte Carlo DNA damage simulations and deterministic repair models to examine putative mechanisms of cell killing. *Radiat Res* 2008;169:447−459.
6. Semenenko VA, Stewart RD. Fast Monte Carlo simulation of DNA damage formed by electrons and light ions. *Phys Med Biol* 2006;51: 1693−1706.
7. Semenenko VA, Stewart RD. A fast Monte Carlo algorithm to simulate the spectrum of DNA damages formed by ionizing radiation. *Radiat Res* 2004;161:451−457.
8. Wilson RR. Radiological use of fast protons. *Radiology* 1946;47: 487−491.
9. Bortfeld T. An analytical approximation of the Bragg curve for therapeutic proton beams. *Med Phys* 1997;24:2024−2033.
10. Wilkens JJ, Oelfke U. Three-dimensional LET calculations for treatment planning of proton therapy. *Z Med Phys* 2004;14:41−46.
11. Bethe H. Zur Theorie des Durchgangs schneller Korpuskularstrahlen durch Materie [On the theory of the passage of fast corpuscular beams through matter]. *Annalen der Physik* 1930;397:325−400.
12. Zaider M, Rossi HH. The synergistic effects of different radiations. *Radiat Res* 1980;83:732−739.
13. Wilkens JJ, Oelfke U. Fast multifield optimization of the biological effect in ion therapy. *Phys Med Biol* 2006;51:3127−3140.
14. Furusawa Y, Fukutsu K, Aoki M, *et al*. Inactivation of aerobic and hypoxic cells from three different cell lines by accelerated (3)He-, (12)C- and (20)Ne- ion beams. *Radiat Res* 2000;154: 485−496.
15. Carlson DJ, Stewart RD, Li XA, *et al*. Comparison of *in vitro* and *in vivo* alpha/beta ratios for prostate cancer. *Phys Med Biol* 2004;49:4477−4491.
16. Girinsky T, Lubin R, Pignon JP, *et al*. Predictive value of *in vitro* radiosensitivity parameters in head and neck cancers and cervical carcinomas: Preliminary correlations with local control and overall survival. *Int J Radiat Oncol Biol Phys* 1993;25:3−7.
17. Stuschke M, Thames HD. Fractionation sensitivities and dose-control relations of head and neck carcinomas: Analysis of the randomized hyperfractionation trials. *Radiother Oncol* 1999;51:113−121.
18. Hsiao Y, Stewart RD. Monte Carlo simulation of DNA damage induction by x-rays and selected radioisotopes. *Phys Med Biol* 2008;53:233−244.
19. Weber U, Kraft G. Design and construction of a ripple filter for a smoothed depth dose distribution in conformal particle therapy. *Phys Med Biol* 1999;44:2765−2775.
20. Grassberger C, Trofimov A, Lomax A, *et al*. Variations in linear energy transfer within clinical proton therapy fields and the potential for biological treatment planning. *Int J Radiat Oncol Biol Phys* 2011;80: 1559−1566.
21. Carabe-Fernandez A, Dale RG, Hopewell JW, *et al*. Fractionation effects in particle radiotherapy: Implications for hypo-fractionation regimes. *Phys Med Biol* 2010;55:5685−5700.
22. Scholz M, Kraft G. Track structure and the calculation of biological effects of heavy charged particles. *Adv Space Res* 1996;18:5−14.
23. Wilkens JJ, Oelfke U. Direct comparison of biologically optimized spread-out Bragg peaks for protons and carbon ions. *Int J Radiat Oncol Biol Phys* 2008;70:262−266.
24. Inaniwa T, Furukawa T, Kase Y, *et al*. Treatment planning for a scanned carbon beam with a modified microdosimetric kinetic model. *Phys Med Biol* 2010;55:6721−6737.